



ARTICLE OPEN



Molecular profiling of the hippocampus of children with autism spectrum disorder

Lindsay E. Rexrode¹, Joshua Hartley¹, Kurt C. Showmaker¹ ², Lavanya Challagundla³, Michael W. Vandewege², Brigitte E. Martin³, Estelle Blair¹, Ratna Bollavarapu¹, Rhenius B. Antonyraj¹, Keauna Hilton¹, Alex Gardiner¹, Jake Valeri^{1,4}, Barbara Gisabella^{1,4}, Michael R. Garrett³, Theoharis C. Theoharides^{5,6} and Harry Pantazopoulos^{1,4} 

© The Author(s) 2024

Several lines of evidence point to a key role of the hippocampus in Autism Spectrum Disorders (ASD). Altered hippocampal volume and deficits in memory for person and emotion related stimuli have been reported, along with enhanced ability for declarative memories. Mouse models have demonstrated a critical role of the hippocampus in social memory dysfunction, associated with ASD, together with decreased synaptic plasticity. Chondroitin sulfate proteoglycans (CSPGs), a family of extracellular matrix molecules, represent a potential key link between neurodevelopment, synaptic plasticity, and immune system signaling. There is a lack of information regarding the molecular pathology of the hippocampus in ASD. We conducted RNAseq profiling on postmortem human brain samples containing the hippocampus from male children with ASD ($n = 7$) and normal male children (3–14 yrs old), ($n = 6$) from the NIH NeuroBioBank. Gene expression profiling analysis implicated molecular pathways involved in extracellular matrix organization, neurodevelopment, synaptic regulation, and immune system signaling. qRT-PCR and Western blotting were used to confirm several of the top markers identified. The CSPG protein BCAN was examined with multiplex immunofluorescence to analyze cell-type specific expression of BCAN and astrocyte morphology. We observed decreased expression of synaptic proteins PSD95 ($p < 0.02$) and SYN1 ($p < 0.02$), increased expression of the extracellular matrix (ECM) protease MMP9 ($p < 0.03$), and decreased expression of MEF2C ($p < 0.03$). We also observed increased BCAN expression with astrocytes in children with ASD, together with altered astrocyte morphology. Our results point to alterations in immune system signaling, glia cell differentiation, and synaptic signaling in the hippocampus of children with ASD, together with alterations in extracellular matrix molecules. Furthermore, our results demonstrate altered expression of genes implicated in genetic studies of ASD including SYN1 and MEF2C.

Molecular Psychiatry; <https://doi.org/10.1038/s41380-024-02441-8>


INTRODUCTION

Autism Spectrum Disorder (ASD) is a developmental condition impacting the global population with increasing prevalence [1]. ASD is characterized by impaired social interactions and communication along with stereotypic movements [2, 3]. The pathogenesis of ASD is unknown, limiting development of therapeutic and preventative strategies. Several lines of evidence point to a key role of the hippocampus in ASD. Altered hippocampal volume and deficits in memory for person and emotion related stimuli have been reported, along with enhanced ability for declarative memories [4, 5]. Specifically, increased hippocampal volume was reported in children and adults with ASD [6]. Preclinical models have demonstrated a critical role of the hippocampus in social memory dysfunction associated with ASD, together with decreased synaptic plasticity [7, 8]. Abnormalities in neurodevelopmental and neuroimmune processes are key features of ASD [9, 10] and may contribute to hippocampal dysfunction. Growing evidence indicates that altered neuroimmune signaling during development is critically involved in ASD [11–16]. Brain imaging and human postmortem studies suggest

that enhanced neuroimmune signaling is present in several brain regions in ASD [12, 13, 16]. Furthermore, a recent single cell RNAseq profiling study of the prefrontal and anterior cingulate cortex implicates several microglial specific molecules [17]. Maternal immune activation results in sex-specific microglial alterations primarily impacting male offspring [14, 15, 18], reflective of the male prevalence of ASD [19]. Brain neuroimmune signaling has several distinctions from classic peripheral inflammatory processes that relate to aspects of ASD [20]. Brain neuroimmune molecules are involved in a range of regulatory processes including synaptic plasticity and neurodevelopmental processes in addition to neuroimmune response [20], which may impact neurodevelopmental and synaptic regulation processes in ASD.

Chondroitin sulfate proteoglycans (CSPGs) and their endogenous proteases are critically involved in mediating immune responses and represent key factors at the intersection of neuroimmune signaling, neurodevelopment, and synaptic regulation. Chondroitin sulfate is a potent inhibitor of immune response (for review see [21]). Several lines of evidence indicate that altered

¹Department of Psychiatry and Human Behavior, University of Mississippi Medical School, Jackson, MS, USA. ²Dasomics LLC, Madison, MS, USA. ³Department of Cell and Molecular Biology, University of Mississippi Medical School, Jackson, MS, USA. ⁴Program in Neuroscience, University of Mississippi Medical School, Jackson, MS, USA. ⁵Institute of Neuro-Immune Medicine, Nova Southeastern University, Clearwater, FL, USA. ⁶Department of Immunology, Tufts University School of Medicine, Boston, MA, USA.

email: cpantazopoulos@umc.edu

Received: 12 October 2022 Revised: 16 January 2024 Accepted: 18 January 2024

Published online: 14 February 2024

neurodevelopment plays a key role in ASD [10, 22, 23]. For example, neuronal and dendritic spine development is altered in the amygdala of children with ASD [9, 10]. Abnormalities in neuronal migration have also been reported [22, 23]. CSPGs are extracellular matrix molecules (ECMs) critically involved in neuronal migration, glial cell maturation, and synaptic stabilization [24–26]. Work from our group and others have reported alterations of ECMs including CSPGs in subjects with schizophrenia [27, 28]. Genetic factors and gene expression pathways implicated in ASD share a degree of overlap with schizophrenia [29, 30]. Recent evidence suggests these disorders may also share alterations in ECMs. Genome-wide association studies (GWAS) implicate several ECM genes in ASD, including genes encoding for endogenous proteases such as ADAMT5, ADAMT5, ADAMT514 [31–35]. Increased levels of the CSPG protease matrix metalloproteinase 9 (MMP9) have been reported in amniotic fluid samples of children with ASD [36].

Despite the critical role of CSPGs in neurodevelopment, neuroimmune signaling and synaptic regulation [21, 37, 38], and evidence for their involvement in several psychiatric disorders [27, 39–41], the role of CSPGs in the brain of children with ASD has not been examined. We propose that CSPGs are shared downstream targets from several genetic and environmental factors that are at the intersection of neurodevelopment, neuroimmune signaling, and synaptic regulation. As a first step in identifying the molecular pathology of the hippocampus in ASD, we conducted RNAseq profiling of human postmortem hippocampus samples from male children with ASD and age matched normotyped control subjects (3–14 yrs old) (Table 1). We focused on a neurodevelopmental time-window encompassing stages of synaptic development and refinement.

METHODS

Human subjects

Postmortem human brain hippocampal samples of ASD ($n = 7$) and non-ASD ($n = 6$) male children (3–14 yrs old, Table 1) were obtained from the NIH NeuroBioBank at the University of Maryland, Baltimore MD which obtained informed consent. IRB approval was obtained from the Univ. of Maryland IRB committee. Cohort size was determined based on previous studies [16]. Available samples for RNA analysis consisted of ASD ($n = 7$) and non-ASD ($n = 6$). For Western Blotting studies, hippocampal protein samples were available from the same subjects along with three additional samples, resulting in ASD ($n = 8$) and non-ASD ($n = 8$) male children (Table 1). Microscopy studies were conducted on a subset of frozen tissue sections from the same subjects consisting of 6 subjects with ASD and 6 control subjects in order to obtain cell type specific data and glial cell morphology information. Sections from the remaining subjects in the cohort did not display suitable cytoarchitecture for microscopy. Frozen blocks were sectioned at 30 μm thickness using a Leica CM 3050 S cryostat (Leica Biosystems, Buffalo Grove, IL). For fluorescent microscopy studies, sections were stained with DAPI to identify hippocampal subregions and to confirm cell specific labeling. This study is limited to males only because ASD is four times more common in males than females, and to avoid any additional sex and hormonal variabilities.

RNAseq profiling. RNA isolation, library preparation, and next generation sequencing was performed by the Molecular and Genomics Core Facility at the University of Mississippi Medical Center, as described previously [42]. Total RNA was isolated from tissue samples using the Invitrogen PureLink RNA Mini kit with Trizol (Life Technologies; Carlsbad, CA, USA) following manufacturer protocol. Quality control of total RNA was assessed using the Qiagen QIAxcel Advanced System for quality and Qubit Fluorometer for concentration measures. The RQI was 6.6 ± 2.1 (mean \pm SD). Libraries were prepared using the TruSeq Stranded Total RNA LT Sample Prep Kit from Illumina (San Diego, CA, USA) per manufacturer's protocol using up to 1 μg of RNA per sample. Libraries were index-tagged, pooled for multiplexing (all 13 samples) and sequencing was performed on the Illumina NextSeq 500 platform using a paired-end read (2 \times 75 bp) protocol with the Illumina 150 cycle High-Output reagent kit.

RNAseq bioinformatics analysis. Differential expression of genes (i.e. mRNA and non-coding RNA) was assessed between subjects with ASD and controls. Reads were aligned to the NCBI GRCh38Decoy Refseq genome with the basespace application RNA-Seq Alignment (Version: 2.0.1 [workflow version 3.19.1.12 + master]) that conducted both splice aware genome alignment with STAR alignment (version 2.6.1a [43]), and transcriptome quantification with Salmon (version 0.11.2 [44]). Differential expression (DE) of the genes (DGE) were conducted with the DESeq2 (1.20.0, [45]) and tximport (version 1.8.0, Sonesson 2015) R packages using the BaseSpace RNA-Seq Differential Expression (version 1.0.1 [Illumina Secondary Analysis Software version 3.18.18.9 + master]) application. A gene was considered differentially expressed if the False Discovery Rate (FDR) adjusted p-value did not exceed 0.05. Heatmap visualizations were generated using the pheatmap (Kolde 2012) function in R based on hierarchical clustering (method = average; distance = correlation) of the 'regularized log' transformation values from DESeq2. Gene Set Enrichment Analysis (GSEA) was conducted with the ClusterProfiler R package [46] using the functions gseGO, gseKEGG, and gsePathway [47] for GO Biological Processes (BP), KEGG, and Reactome geneset collections, respectively, each with the parameters pAdjustMethod = "BH", pvalueCut-off = 0.05, minGSSize = 20, and maxGSSize = 500. Plots were generated with R packages ggplot2 (Wickham 2016) and pheatmap (Kolde 2012). Raw sequenced reads were deposited into the NIH Data Archive Collection (C3917: experiment ID:2219 :<https://doi.org/10.15154/1528650>).

qRT-PCR. Total RNA (0.5 μg) was used as a template for synthesis of cDNA in a total reaction volume of 20 μl using Invitrogen iScript™ Advanced cDNA synthesis kits (cat# 1725038, Invitrogen, Grand Island, NY). Twenty-eight transcripts identified as differentially expressed in RNAseq studies were chosen for validation as well as the downstream protease MMP9 and the neuroimmune signaling molecule IL1B. B2M and ACTB were used as reference genes. Pre-validated qPCR probes from Bio-Rad PrimerPC were used (see Supplementary Table 2). qPCR was performed using 384 well plates with the Bio-Rad CFX 384 real-time PCR detection system and iQ-SYBR Green Supermix (cat# 1708880, Bio-Rad, Hercules, CA). PCR reactions contained 10 μl of the SYBR Green PCR mix, 0.04 μl of 100 μM forward and reverse primers, 1 μl of cDNA, in a final volume of 20 μl using nuclease free water. For all primer pairs, PCR cycling conditions were 50 °C for 2 min and 95 °C for 2 min, followed by 50 cycles of 95 °C for 15 s, 60 °C for 15 s and 72 °C for 1 min. PCR product quantification was performed by the relative quantification method [48, 49] and expressed as standardized arbitrary units [48].

Western blot analysis. Protein levels of MMP9, IL1 β , PSD-95, SYN1, MEF2C, and DGCR6 were determined by Western blotting analysis. Brain tissues were homogenized using lysis radio-immuno precipitation (RIPA) buffer in the presence of a protease inhibitor cocktails (Sigma- Aldrich, St. Louis, MO), followed by sonication using a Polytron (Brinkmann Instruments, Westbury, NY). Total protein concentration was determined by bicinchoninic acid assay (Thermo Fisher Scientific, Waltham, MA) with bovine serum albumin (BSA) as standard. The total cellular protein (30 μg aliquots) was separated using Biorad 4–15% MP TGX Stain-Free gels under SDS denaturing conditions (Biorad, Hercules, CA) and electrotransferred onto Biorad LF PVDF membranes (Biorad, Hercules, CA) using Biorad rapid transfer kits. Blocking was carried out using Biorad EveryBlot blocking buffer with 0.01% Tween-20 (Biorad, Hercules, CA). The membranes were probed with the following primary antibodies: rabbit anti-MMP9 (1:1000 μl , cat#AB13458, MilliporeSigma, Burlington, MA), rabbit anti-PSD-95 (1:500 μl , cat#20665-1-AP, Protein Tech, Rosemont, IL), rabbit anti-SYN1 (1:500 μl , cat#20258-1-AP, Protein Tech, Rosemont, IL), rabbit anti-MEF2C (1:500 μl , cat#10056-1-AP, Abnova, Taipei City, Taiwan), DGCR6 (1:500 μl , cat#H00008214-B01P, Protein Tech, Rosemont, IL) using VCP for the loading control (mouse anti-VCP, Santa Cruz Biotechnology cat# sc-57492 and rabbit anti-VCP, Abcam Inc. cat# ab111740) according to prior studies [50]. All proteins were visualized with Biorad anti-mouse Starbright blue 520 and anti-rabbit Starbright blue 700 fluorescence secondary antibodies (Biorad, Hercules, CA). Blots were imaged on a Biorad ChemicDoc MP Imaging system and analyzed using Biorad Image Lab v 6.0.1 (Biorad, Hercules, CA).

Immunohistochemistry. Triple immunofluorescence labeling was performed using primary antibodies for the target proteins rabbit anti-MMP9 (1:500 μl , cat#AB13458, MilliporeSigma, Burlington, MA), rabbit anti-BCAN (1:500 μl , cat#19017-1-AP, Protein Tech, Rosemont, IL) biotinylated Wisteria floribunda agglutinin lectin (1:1000 μl , cat# B-1355, Vector Labs, Burlingame, CA), mouse anti-IBA1 (1:1000 μl , Wako Chemicals, cat#

Table 1. Subjects and demographic information.

Subject	Age	Sex	Race	RIN	PMI (hrs)	Hemisphere	Epilepsy	Cause of Death	Measures (RNAseq + qPCR, Western, Microscopy)
Control subjects									
4332	5	Male	Black	7.4	18	Left	No	Natural	Western
4337	8	Male	Black	8.4	16	Left	No	Natural	RNA, Western, Microscopy
4925	13	Male	Black	6.8	16	Left	No	Natural	RNA, Western, Microscopy
5170	13	Male	Black	6.8	20	Left	No	Undetermined	RNA, Western, Microscopy
5334	12	Male	Hispanic	2.4	15	Left	No	Not available	RNA, Western, Microscopy
5387	12	Male	White	7.5	13	Left	No	Accidental	Western
5391	8	Male	White	6.9	12	Left	No	Accidental	RNA, Western, Microscopy
5408	6	Male	Black	7.6	16	Left	No	Accidental	RNA, Western, Microscopy
	Mean ± SD	8 M	5B, 2W, 1H	6.7±1.8	15.8±2.5	8 Left	8 No		
	9.6 ± 3.25								
ASD subjects									
4231	8	Male	N/A	7.1	12	Left	N/A	N/A	RNA, Western
4334	8	Male	Hispanic	7.1	27	Left	No	Natural	RNA, Western, Microscopy
4849	7	Male	Black	6.7	20	Left	No	Accidental	Western
5144	7	Male	White	7.7	3	Left	No	Natural	RNA, Western, Microscopy
5308	4	Male	White	6.0	21	Left	No	Accidental	RNA, Western, Microscopy
5454	11	Male	N/A	4.8	20	Left	N/A	N/A	RNA, Western, Microscopy
5565	12	Male	Black	8.3	22	Left	Yes	Natural	RNA, Western, Microscopy
5841	12	Male	N/A	6.5	15	Left	N/A	N/A	RNA, Western, Microscopy
	Mean ± SD	8 M	2B, 2W, 1H, 3 N/A	6.8±1.1	17.5 ± 7.4	8 Left	4 No, 1 Yes, 3 N/A		
	8.6 ± 2.83								

013-27593), rabbit anti-IBA1 (1:1000 μ l, Wako Chemicals cat#019-19741), or mouse anti-TPSAB1 (1:500 μ l, cat#66174-1-Ig, Protein Tech, Rosemont, IL). Sections were post-fixed in 4% PFA for 30 min, and then co-incubated in primary antibodies in 2% bovine serum albumin (BSA) for 72 h at 4 °C. This step was followed by 4 h incubation at room temperature in Alexa Fluor goat anti-mouse 647 (1:300 μ l; A-21235, Invitrogen, Grand Island, NY) and donkey anti-rabbit 555 (1:300 μ l; A-32794, Invitrogen, Grand Island, NY), followed by 2 min in TrueBlack solution for autofluorescence quenching (Biotum, cat#23007) [51, 52]. Sections were mounted and coverslipped using Dako mounting media (S3023, Dako, North America, Carpinteria, CA). All sections were coverslipped and coded for quantitative analysis blinded to diagnosis. Sections from all brains included in the study were processed simultaneously to avoid procedural differences. Omission of streptavidin or omission of the primary or secondary antibodies were used as negative controls.

Microscopy quantification. Sections containing the hippocampus were quantified using an Olympus BX 61 fluorescent microscope interfaced with StereoInvestigator v11 (MBF Biosciences, Williston, VT). Borders of each subregion were defined according to the Allen Brain Atlas and traced under 4 \times magnification. Each traced region was systematically scanned through the full x, y, and z-axes under 40 \times magnification to count each immunolabeled cell.

Sholl analysis. Fluorescent multichannel images were systematically sampled from CA4 of glial fibrillary acidic protein (GFAP) labeled glial cells with or without BCAN expression and captured using a 60 \times oil objective (369 glial cells from subjects with ASD and 419 glial cells from control subjects obtained from 6 ASD subjects and 6 control subjects) using StereoInvestigator v 11.0 (MBF Biosciences, Williston, VT). Images were analyzed using the Sholl analysis probe in NeuroLucida 360 (MBF Biosciences, Williston, VT).

Numerical densities of immunoreactive cells. Numerical densities were calculated as $Nd = \Sigma N / \Sigma V$ where N = sum of all cells counted in each region, and V is the volume of each region, calculated as $V = \Sigma a \cdot z$, where z is the thickness of each section (30 μ m) and a is area in μ m².

Statistical analysis. Stepwise linear regression analysis of covariance was applied to the main outcome qRT-PCR, Western blotting, and microscopy measures to test differences between ASD and control groups and effects of confounding variables including age, PMI, RIN, race, history of epilepsy, and cause of death. Logarithmic transformation was applied to values when not normally distributed. Potential effects of these confounding covariates were tested on our outcome measures in stepwise linear regression analysis, as conducted previously [53] using JMP Pro v15.1.0 software (Cary, North Carolina). Significance of comparisons by ANOVA is denoted by $p < 0.05$. No information was available on severity of ASD, any comorbidities or the effects of any therapeutic drugs in the ASD group.

RESULTS

RNAseq profiling

RNAseq gene expression profiling identified 2851 differentially expressed genes in the hippocampus of children with ASD, including genes implicated in genetic analysis studies [53–56] and genes involved in synaptic regulation, blood vessel and blood-brain barrier regulation, immune signaling, ECM organization, and calcium channel activity (Fig. 1, Supplementary Fig. 1, and Supplementary Table 1).

Pathway analysis identified upregulation of pathways involved in immune and inflammatory response (ex:R-HSA-877300; GO0006959), vasculature regulation (ex:hsa04610) and ECM organization (ex: R-HSA-1474244) (Fig. 1, Supplementary Fig. 1, and Supplementary Table 1). We identified downregulation of several pathways involved in synaptic signaling and synaptic transmission (ex:GO0099504; R-HSA-112314) (Fig. 1, Supplementary Figs. 1, 2, and Supplementary Table 1). Hierarchical cluster analysis revealed expression variability among subjects and DEGs (Fig. 2A). However, there was noticeable separation between control and ASD subjects among ECMs, ECM proteases, and synaptic signaling molecule

genes, but weaker clustering among genes related to immune signaling (Fig. 2B–E).

qRT-PCR confirmation of DEGs

qRT-PCR on a subset of differentially expressed genes (DEGs) confirmed several of the top DEGs. Genes highly expressed in the hippocampus of children with ASD included IL1RL1, MMP9, OTX2 and SERPIND1 (Fig. 3A). Increased expression was also detected for several additional ECMs including ADAMTSL4, CHST3, MMP14 and VCAN, and decreased expression for ADAM23, ADAMTS3, SEMA3E, and SPOCK1 (Fig. 3B). Decreased expression was observed for CACNA1I, whereas expression for additional calcium channels and IL1beta approached significance (Fig. 3C). Decreased expression was confirmed for the genetically associated markers SYN1 and ADCYAP1 (Fig. 3D), whereas DGRC6 and RSPO1 did not approach significance between groups. Decreased expression was confirmed for most of the synaptic markers examined (Fig. 3E).

Western blotting protein confirmation of DEGs

Western blotting on several of the top candidates confirmed gene expression measures with protein levels. The active and cleaved forms of MMP9 were increased in children with ASD whereas the precursor form was not significantly different between the two groups (Fig. 4A–C). The 17 and 30 kDa isoforms of IL1beta protein were both significantly greater in children with ASD compared to age matched control subjects (Fig. 4D, E). Furthermore, decreases in the synaptic proteins PSD95 and SYN1 were observed in subjects with ASD (Fig. 4F–H). A significant decrease in protein expression was observed for MEF2C (Fig. 4I) but not for DGRC6 (Fig. 4J).

MMP9 expression in microglia, neurons and mast cells

MMP9 labeling in the hippocampus was observed primarily in microglia as well as a small percentage of neurons and cells displaying mast cell morphology. Tryptase alpha/beta1 (TPSAB1) labeling was used to confirm the presence of mast cells in the human hippocampus of subjects with ASD and control subjects (Supplementary Fig. 3A–C). Immunofluorescence confirmed that MMP9 expression colocalized with mast cells (Supplementary Fig. 3D) and microglial cells labeled with IBA1 (Supplementary Fig. 3E). Densities of MMP9 labeled mast cells were not altered in the DG or CA4 of subjects with ASD compared to control subjects (Supplementary Fig. 3F–H).

Increased BCAN expression in GFAP+ astrocytes in children with ASD

Brevican (BCAN) expression was observed in cells with astrocytic morphology, and 20–30% of these GFAP cells displayed co-expression of BCAN (Supplementary Fig. 4A, B). Quantification of BCAN+ and GFAP+ cells in the CA4 area of the hippocampus revealed increase density of GFAP cells co-expressing BCAN (Supplementary Fig. 4C). Densities of cells expressing BCAN only or GFAP only were not altered between groups, suggesting that a greater percentage of GFAP cells express BCAN in children with ASD. Statistical comparison of the percentages of GFAP cells expressing BCAN between groups provides additional support for increased expression of BCAN in GFAP cells in children with ASD (Supplementary Fig. 4F).

Altered astrocyte morphology in the hippocampus of children with ASD

Sholl analysis was performed on images systematically sampled from CA4 of GFAP labeled glial cells with or without BCAN expression (369 glial cells from subjects with ASD and 419 glial cells from control subjects obtained from 6 subjects per group) in order to test the hypothesis that astrocytes expressing BCAN display morphological features characteristic of immature glial cells. Glial cells were traced using the Sholl analysis probe in

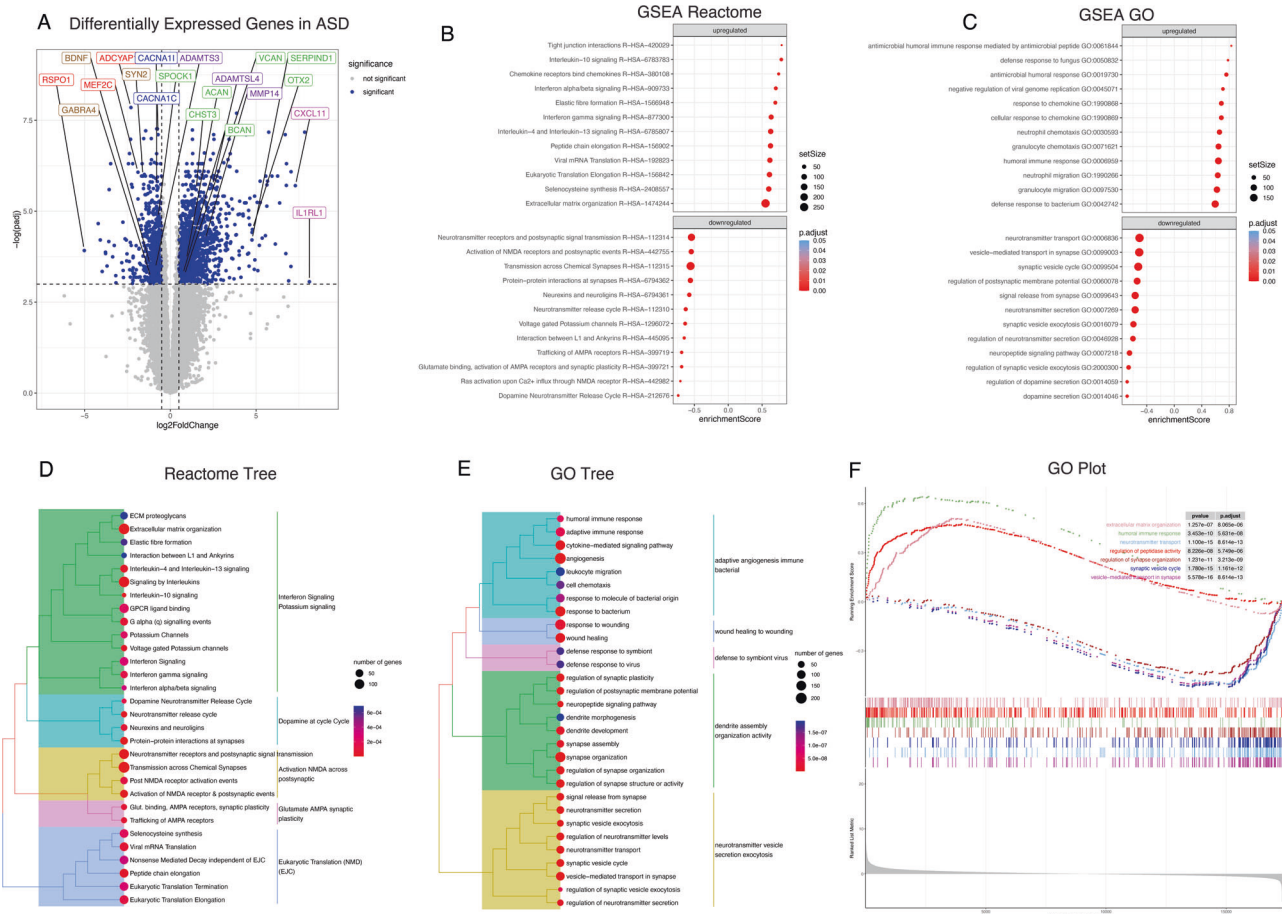


Fig. 1 Differential gene expression pathways in the hippocampus of children with ASD. **A** Volcano plot of DGE: ASD vs. non-ASD controls. On the x-axis is log fold change of genes in subjects with ASD compared to controls, points to the right of 0 represent genes that are increased, and points to the left of 0 genes that are decreased, in ASD compared to controls. Statistical significance is displayed on the y-axis, and $p < 0.05$ are labeled in blue. Select genes with both high fold change and significance are labeled. The top dozen GSEA Reactome analysis identified upregulated pathways, (including extracellular matrix organization and immune signaling pathways), and downregulated pathways involved in synaptic regulation in children with ASD (**B**). Similar top pathways were detected with GSEA GO BP analysis (**C**). Reactome tree and GO tree plots of pathways altered in children with ASD (**D**, **E**). GSEA GO enrichment plot of upregulated and downregulated pathways in children with ASD (**F**).

NeuroLucida 360 (Supplementary Fig. 5A, B) and branches were quantified for measures of branch intersections, length, surface area, volume, diameter, nodes and endings (Supplementary Fig. 5C). In control subjects, GFAP astrocytes co-expressing BCAN had significantly fewer branch intersections along with decreased branch length, surface area, volume and diameter (Supplementary Fig. 5D–J). In comparison, GFAP astrocytes co-expressing BCAN from subjects with ASD had fewer branch intersections, nodes, and endings, along with decreased branch length (Supplementary Fig. 5K–P). Direct comparison between ASD and control subjects revealed increased branch nodes and endings in GFAP only astrocytes in children with ASD compared to decreased branch nodes and endings in GFAP astrocytes co-expressing BCAN (Fig. 4). A significant interaction between age and diagnosis was observed for branch intersections across all astrocytes examined, resulting in an opposite correlation of age with branch intersections in children with ASD compared to non-ASD control subjects (Fig. 4Q).

DISCUSSION

Our results represent, to our knowledge, the first evidence for molecular abnormalities in the hippocampus of children with ASD. We detected gene expression differences between ASD and

control subjects and many changes linked to ECM regulation, neuroimmune signaling, and decreased synaptic signaling are in line with growing evidence for neuroimmune signaling [11–16] and synaptic pathology in ASD [10, 17, 55, 57, 58]. Our results highlight the potential involvement of ECMs with these pathways during a window of neurodevelopment in the hippocampus of children with ASD. Cluster analysis displayed the expected variability in subjects with ASD but suggests that ECMs and synaptic signaling molecules encompass a larger group of subjects than neuroimmune molecules. Furthermore, our data suggest that altered expression of the ECM BCAN may be associated with glial cell maturation deficits in ASD. Several genes implicated by genetic studies on ASD, including MEF2C and SYN1 [54, 55, 58, 59], displayed altered expression in our study, suggesting that these genetic factors may in part contribute to molecular pathology in the hippocampus of children with ASD.

Extracellular matrix molecules

Gene pathways involved in ECM organization were upregulated in the hippocampus of children with ASD (Fig. 1; Reactome pathway), together with mRNA and protein expression changes confirmed with qRT-PCR and Western Blotting for several ECMs (Figs. 3 and 4). CSPGs and their endogenous proteases are critically involved in mediating neurodevelopment, synaptic

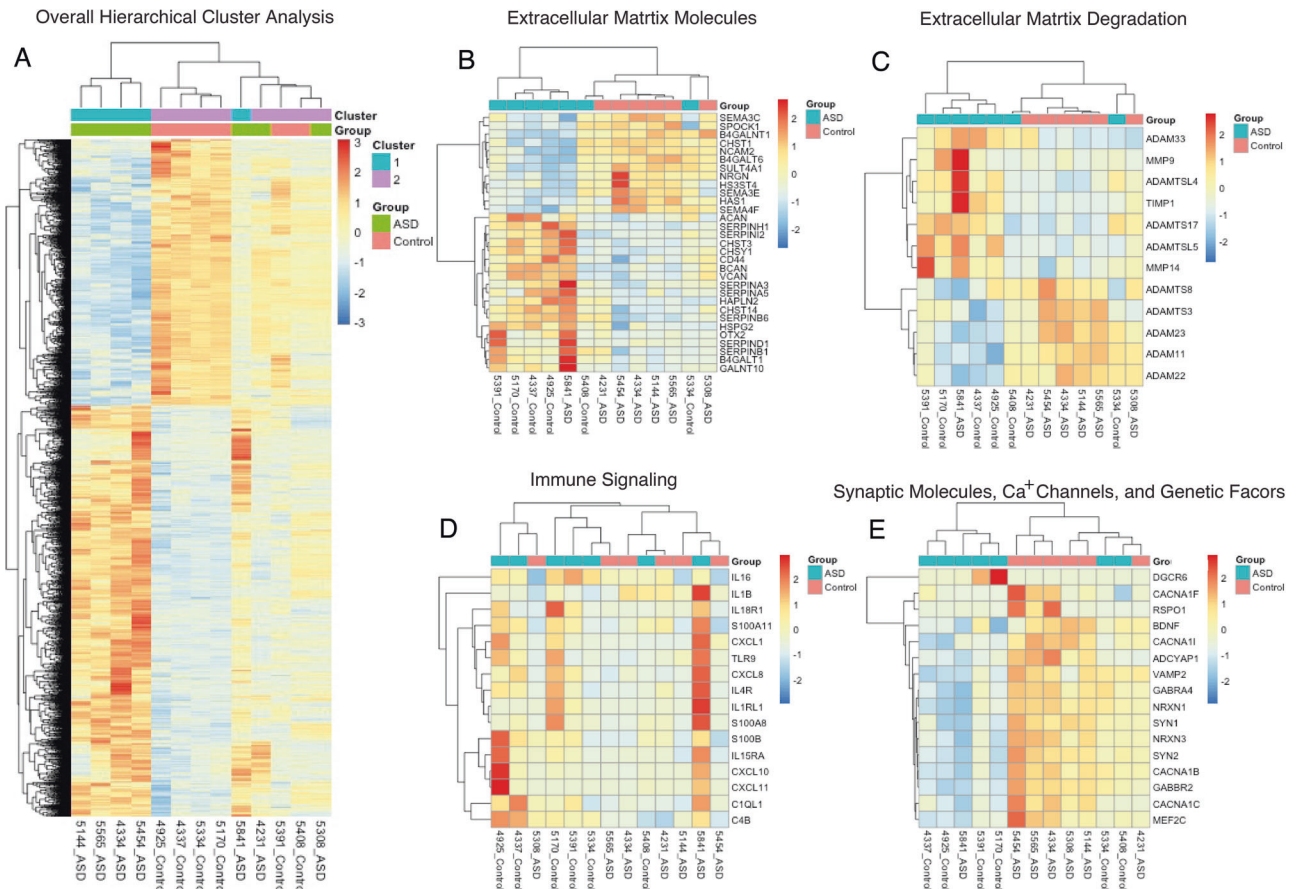


Fig. 2 Hierarchical cluster analysis. **A** Hierarchical and K means clustering of 7 ASD and 6 non-ASD control subjects using regularized log expression of 2851 genes differentially expressed between ASD and non-ASD control subjects in the hippocampus (p -adjusted <0.05). Hierarchical clustering of differentially expressed genes for extracellular matrix molecules (**B**), extracellular matrix degradation molecules (**C**), immune signaling (**D**), and synaptic molecules and genetic factors (**E**).

regulation, and neuroimmune signaling, and thus represent key factors at the intersection of these processes in ASD.

Several ECMs upregulated in children with ASD may contribute to neuroimmune signaling processes. Chondroitin sulfate (CS) is a potent inhibitor of immune response [21, 38] and also inhibits human mast cells [60], activation of which has been implicated in ASD [61]. CS protects from inflammatory neurodegeneration and promotes CNS repair [62, 63]. Genetic reduction of chondroitin sulfate synthase 1 (CHSY1) causes neuroinflammation and neurodegeneration in the mouse hippocampus [38]. Increased expression of ECM proteases may also contribute to enhanced neuroimmune signaling and blood-brain barrier permeability. The endogenous CSPG proteases matrix metalloproteinases (MMPs) are critically involved in promoting neuroimmune signaling [64, 65]. Increased levels of the CSPG protease matrix metalloproteinase 9 (MMP9) have been reported in amniotic fluid samples of children with ASD [36]. MMPs, including MMP9, are primarily produced by astrocytes and microglia in the brain [66, 67]. MMP9 is also produced by mast cells [68, 69], and our data shows MMP9 expression predominantly in microglia and to a lesser extent in neurons and mast cells in the hippocampus of children with ASD (Supplementary Fig. 2).

Evidence from animal models supports the hypothesis that increased MMP9 expression during development contributes to decreased perineuronal nets (PNNs) and synaptic destabilization [70–72]. PNNs are ECM structures that develop around fast-firing neurons and stabilize synaptic plasticity [70–73]. Fragile-X syndrome is a monogenetic disease in which approximately 30% of patients display symptoms of ASD. Several animal models of Fragile-X

syndrome show increased MMP9 expression and reductions of PNNs in the amygdala, auditory cortex and hippocampus, together with impaired fear memory [70–73]. Pharmacological inhibition of MMP9 during development or genetic reduction of MMP9 in these mice restores PNN levels and reduces anxiety [70, 71], supporting the hypothesis that elevated MMP9 during development reduces CSPGs, impairs PNN development and in turn destabilizes synapses during this developmental window.

Altered expression of ECMs may also contribute to neurodevelopmental dysfunction in ASD. For example, VCAN, which encodes the core CSPG protein versican, promotes synaptic maturation during development [74], as well as neuronal differentiation and neurite outgrowth [75]. CHST3, which was also upregulated in ASD, encodes the enzyme involved in chondroitin 6 sulphation and promotes hippocampal synaptic plasticity and memory [76]. Our observed decreased expression of the chondroitin-heparan sulfate proteoglycan SPOCK1 in the hippocampus of children with ASD may contribute to neurodevelopmental dysfunction. SPOCK is highly expressed during brain development in areas of neuronal migration and axonal outgrowth, as well as in synaptic fields [77]. We previously observed decreased SPOCK1 and SPOCK3 mRNA expression in the brain of subjects with schizophrenia [78], which shares genetic overlap with ASD [79]. Furthermore, decreased SPOCK expression was correlated with decreased cognitive function in subjects with schizophrenia [78], suggesting that decreased SPOCK expression may be associated with cognitive function in ASD.

Increased expression of CSPGs may be a compensatory effect to increases in ECM proteases. Increased expression of CSPGs

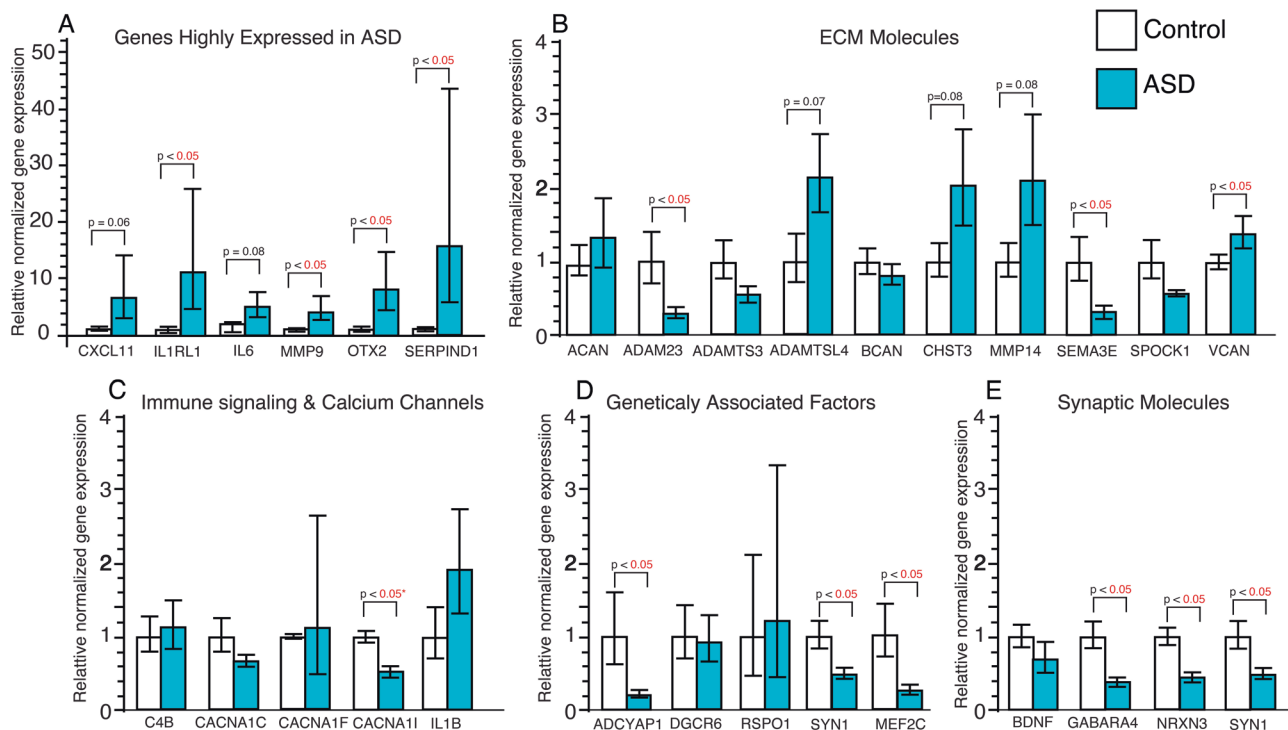


Fig. 3 qPCR confirmation of differentially expressed genes. qPCR analysis was conducted on a subset of 28 genes with differential expression from our RNAseq analysis as well as the downstream extracellular matrix protease MMP9 and the neuroimmune signaling gene IL1B. Significantly increased expression was detected for genes highly expressed in the hippocampus of children with ASD (A). Altered expression was confirmed for several extracellular matrix molecules (B) and the L-type Ca channel CACNA1I (C). Altered gene expression was also confirmed for several genes implicated as genetic factors for ASD (D) and for synaptic molecules (E). *adjusted for significant effects of age and PMI. Significance values are derived from stepwise linear regression models. Bar graphs depict the mean (histogram) and 95% confidence intervals (black lines).

may also reflect their roles in neurodevelopmental processes such as cell maturation, as suggested by our data on BCAN expression in astrocytes. For example, BCAN is expressed in rat hippocampal astrocytes as they mature [80], suggesting BCAN expression promotes astrocyte development. Our observed increase of BCAN positive astrocytes in children with ASD together with impaired astrocyte morphology suggests that increased expression of CSPGs may be associated with immature glial cells in the hippocampus of children with ASD (Fig. 5, Supplementary Figs. 4 and 5).

Synaptic signaling

Our observed decreased gene expression in several pathways involved in synaptic regulation (Fig. 1 and Supplementary Figs. 1 and 2), as well as decreased mRNA and protein expression of synaptic markers together indicate decreased synaptic signaling in the developing hippocampus of children with ASD. We observed decreased protein expression of the synaptic marker PSD-95 (Fig. 4), which has been associated with NMDA receptor alterations and spine changes in ASD [57]. Alterations in synaptic proteins suggest that synaptic alterations in the developing brain of children with ASD may arise from genetic factors such as reported genetic mutations for SYN1 associated with ASD [55]. Evidence that loss of function genetic mutations in SYN1 have been associated with ASD and epilepsy [55], and SYN1 knockout mice display impaired social behaviors and repetitive behaviors [58], supports this possibility. In addition, the observed increase of MMP9 expression and decreased expression of the synaptic markers PSD95 and SYN1 in the same cohort (Fig. 4), suggests that increased MMP9 in the developing brain of children with ASD may contribute to reductions of CSPGs that are involved in stabilizing synapses.

Molecules implicated as genetic factors in ASD

Several molecules implicated as genetic factors for ASD, including MEF2C, SYN1, DGCR6, displayed significantly altered gene expression in our RNAseq analysis. MEF2C and SYN1 decreased expression was also confirmed with qRT-PCR and Western blotting. MEF2C haploinsufficiency has been associated with ASD as well as epilepsy and intellectual disability [54, 59, 81, 82]. Furthermore, mouse models of MEF2C haploinsufficiency demonstrate that impaired MEF2C function results in social deficits, reduced ultrasonic vocalization, hyperactivity, repetitive behavior, and synaptic regulation through both neuronal and microglial cells [54, 83]. Our findings for decreased gene and protein expression of MEF2C in the hippocampus of children with ASD provide the first evidence for altered MEF2C expression in this region in ASD and support the involvement of MEF2C in this disorder. These results also suggest that MEF2C haploinsufficiency may contribute in part to several of the altered molecular pathways observed in our study. Genetic mutations in SYN1 resulting in loss of function have also been associated with ASD and epilepsy [55]. Our observed decrease in SYN1 mRNA and protein expression suggests that SYN1 mutations may in part contribute to decreased SYN1 expression in the hippocampus of children with ASD.

DGCR6 has also been implicated as a genetic factor in ASD as part of the 22.q.11.22 deletion syndrome [56] and was one of the top DEGs in our RNAseq analysis (Supplementary Table 1). However, qRT-PCR and Western blotting measures did not detect changes in DGCR6 protein expression in the hippocampus of children with ASD (Figs. 3 and 4). This may be due in part to the fact that RNAseq evaluates data across the entire transcript/gene and qRT-PCR only evaluates a single region of the gene that may not take into account possible splice variants. Genome-wide

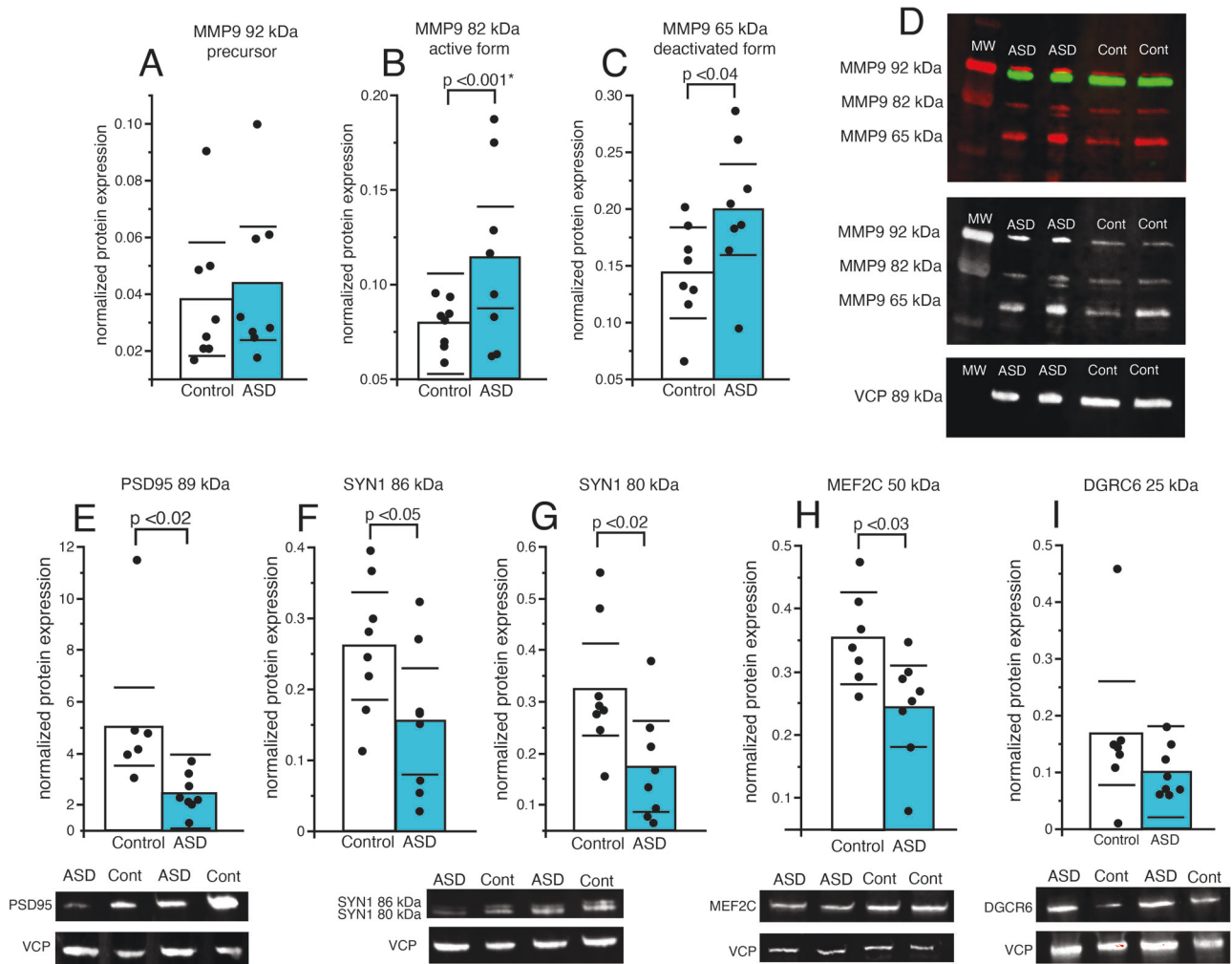


Fig. 4 Protein analysis of MMP9, synaptic markers and genetically associated molecules. Western blot analysis was conducted on the extracellular matrix protease MMP9 and the synaptic markers PSD95 and SYN1, as well as the genetically associated molecules MEF2C and DGRC6. **A** No difference was observed for the 92 kDa isoform of MMP9, whereas expression of the 82 kDa (**B**) and 65 kDa (**C**) isoforms were increased in children with ASD. **D** Representative Western blots of MMP9. Expression of the broad postsynaptic marker PSD95 was decreased in children with ASD (**E**), along with decreased expression of the 86 kDa (**F**) and 80 kDa (**G**) isoforms of the synaptic marker SYN1. Expression of MEF2C, a molecule associated with ASD in genetic studies, was significantly decreased in children with ASD (**H**), whereas no difference was observed for expression of genetically associated molecule DGRC6 (**I**). Significance values are derived from stepwise linear regression models. Bar graphs depict the mean (histogram), black circles depict values for each subject and black lines the 95% confidence intervals.

association studies (GWAS) implicate several ECM genes in ASD, including genes encoding for endogenous proteases such as ADAMTS3, ADAMTS5, ADAMTS14 [32–35], suggesting that genetic factors in ECMs may contribute to the broad ECM gene expression changes we observed in children with ASD.

Neuroimmune signaling

Neuroimmune molecules in the brain are key mediators of regulatory processes including synaptic plasticity and neurodevelopmental processes [20]. Our findings of altered hippocampal neuroimmune signaling pathways may represent aspects of synaptic alterations and neurodevelopmental processes disrupted in children with ASD. These findings are in line with several studies suggesting a critical role for neuroimmune signaling during development in ASD, potentially contributing to synaptic abnormalities [10, 11, 13, 14, 16, 55]. Increased cytokine levels during early developmental stages are associated with increased risk of developing ASD [84, 85]. Rodent models of ASD suggest that maternal immune activation and early postnatal neuroimmune signaling contribute to synaptic dysfunction in several brain regions [15, 86], including the hippocampus [87, 88]. Our findings

for increased gene expression in inflammatory signaling pathways provide support for the involvement of neuroimmune signaling in the developing hippocampus of children with ASD. Several genes with significantly increased expression in our study have recently been implicated in astrocyte response to inflammation, including CXCL10, GBP2, TIMP1, SPERPINA3 [89]. Several of these molecules including CXCL10, TIMP1 and well as IL1RL1 have been demonstrated to impact synaptic plasticity [90–93]. ECMs are intricately involved with neuroimmune signaling in the regulation of neurodevelopmental processes and synaptic plasticity. A recent single cell RNAseq profiling study in postmortem samples of subjects with ASD implicated microglial alterations in ASD [17]. These changes consisted of altered expression of ECMs involved in neurodevelopmental and synaptic regulation, including increased expression of the CSPG sulfotransferase CSGALNACT1 in microglia, and increased expression of the endogenous CSPG proteases MMP16 and ADAMTS9 [17]. Furthermore, microglial signaling through the IL1RL1 receptor regulates hippocampal synaptic plasticity through ECM remodeling [93], providing further support that neuroimmune signaling molecules altered in children with ASD may impact ECM and synaptic molecules. Altered neuroimmune

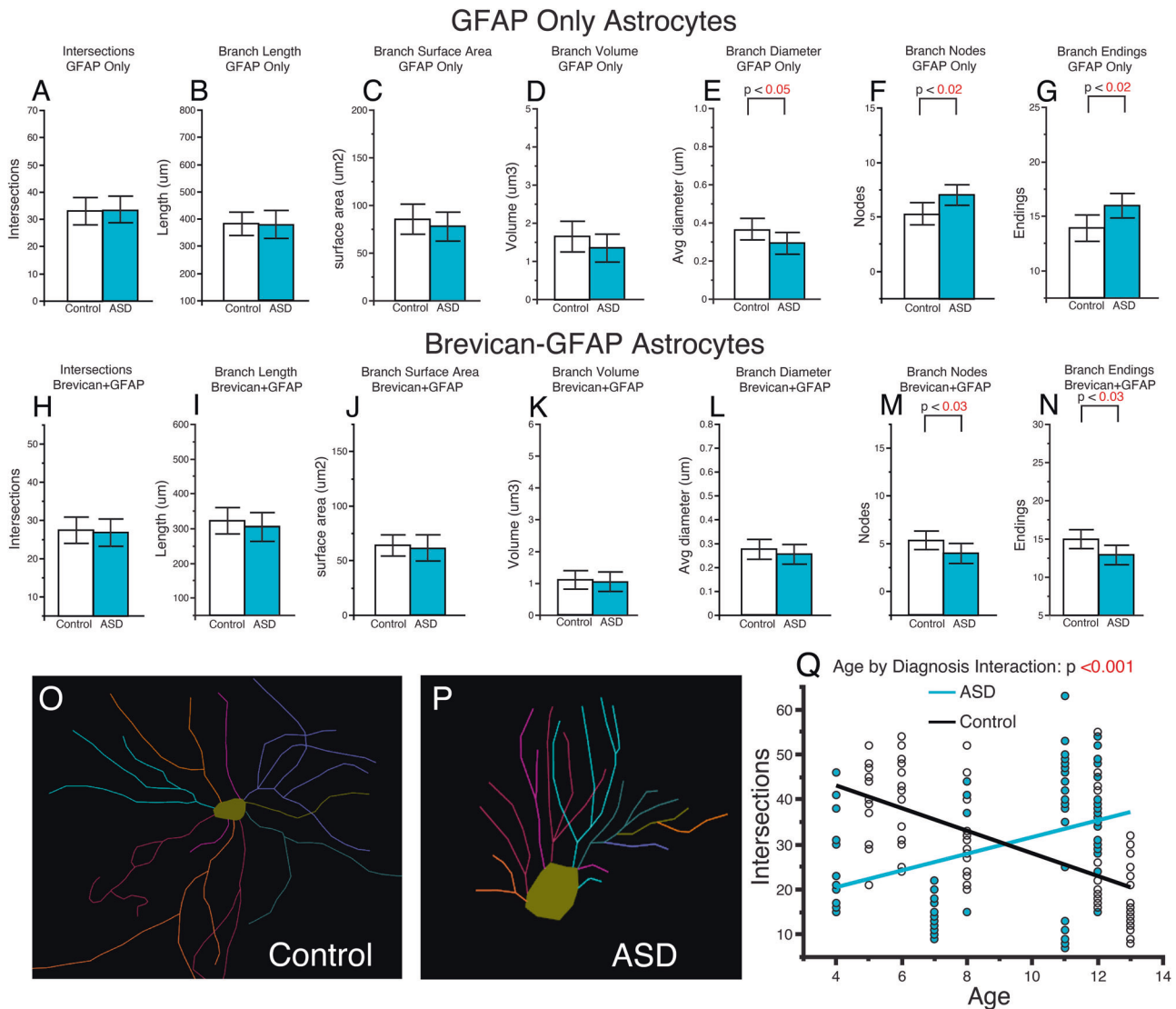


Fig. 5 Altered astrocyte morphology in the hippocampus of children with ASD. Sholl analysis was conducted on a subset of samples from children with ASD and non-ASD control subjects ($n = 6/\text{group}$). **A** No differences in branch intersections, branch length, surface area, or volume, were observed between diagnosis groups for astrocytes expressing GFAP only (**A–D**). A significant decrease was observed for branch diameter (**E**) together with an increase in branch nodes and endings (**F, G**) for GFAP only astrocytes in children with ASD. No differences were detected for branch intersections, branch length, surface area, volume, or diameter for astrocytes co-labeled with GFAP and BCAN (**H–L**). Branch nodes and endings were significantly decreases in GFAP-BCAN astrocytes from children with ASD (**M, N**). Representative tracings of a GFAP-BCAN astrocyte from a control subject (**O**) and a subject with ASD (**P**). Branch intersections across all astrocytes displayed a significant interaction between age and diagnosis, resulting in a negative correlation of intersections by age in control subjects compared to a positive correlation in subjects with ASD (**Q**). Blue circles represent values from subjects with ASD, white circles represent values from control subjects. Significance values are derived from stepwise linear regression models. Bar graphs depict the mean (histogram) and 95% confidence intervals (black lines).

signaling thus may be at the intersection of immune signaling, synaptic plasticity and neurodevelopmental processes in the hippocampus of children with ASD.

Blood-brain barrier regulation

Gene pathways involved in regulation of blood vessels were upregulated in children with ASD in our study (Fig. 1: angiogenesis GO pathway; Supplementary Fig. 1 and Supplementary Table 1). Furthermore, ECMs are also highly involved in blood-brain barrier (BBB) regulation [94]. Our findings suggesting altered BBB composition in the hippocampus of children with ASD are in line with recent evidence for BBB dysfunction in ASD [95, 96]. Altered expression of genes involved in BBB integrity were reported in postmortem cortex and cerebellum samples from subjects with

ASD, together with increased expression of MMP9 and neuroimmune signaling molecules [96]. Mutations in CHD7 have been associated with ASD and may contribute to changes in BBB glial cells that impact serotonin signaling and sleep defects [95]. CHD7 gene expression was significantly upregulated in our RNAseq dataset (Supplementary Table 1). SERPIND1, upregulated in our dataset in children with ASD, is involved in promoting vascular endothelial function and angiogenesis [97], and is activated by glycosaminoglycans [98]. Furthermore, a recent report demonstrated that decreased SPOCK1 expression results in increased BBB leakage in the developing mouse brain [99]. We observed decreased SPOCK1 mRNA in hippocampal samples from children with ASD (Figs. 1 and 3), suggesting that impaired SPOCK1 expression may contribute to BBB dysfunction in this disorder.

Speculatively, our observed changes in ECM signaling pathways may contribute to altered BBB permeability and in turn increased neuroimmune signaling in the hippocampus of children with ASD.

Technical considerations

Our study consisted of bulk hippocampal gene and protein expression analyses, which does not allow for analysis of expression changes in specific hippocampal subfields or anterior to posterior gradients in expression. Furthermore, our bulk hippocampal profiling approach did not allow for evaluation of cell type specific changes. Future studies consisting of hippocampal subregion specific profiling and larger numbers of subjects may provide greater information regarding the hippocampal neurocircuitry alterations in children with ASD.

In summary, our results provide evidence regarding molecular alterations in the hippocampus of children with ASD during a key neurodevelopmental period. These findings point to ECM abnormalities at the intersection of gene expression pathways involved in synaptic regulation, blood-brain barrier regulation, and neuroimmune signaling. Several factors implicated in genetic studies of ASD including MEF2C and SYN1 displayed altered gene expression in our study and suggest that alterations in signaling pathways involved in ECM, neuroimmune signaling and synaptic regulation may be downstream from multiple genetic factors in ASD.

DATA AVAILABILITY

Gene expression profiling data will be publicly available on NCBI dbGaP upon manuscript publication. All other data are available in the main text or supplementary materials.

REFERENCES

- Solmi M, Song M, Yon DK, Lee SW, Fombonne E, Kim MS, et al. Incidence, prevalence, and global burden of autism spectrum disorder from 1990 to 2019 across 204 countries. *Mol Psychiatry*. 2022;27:4172–4180.
- Lai MC, Lombardo MV, Baron-Cohen S. Autism. *Lancet*. 2014;383:896–910.
- Prevention CFDA. CDC estimates 1 in 59 children has been identified with autism spectrum disorder; <https://www.cdc.gov/features/new-autism-data/index.html>, 2018.
- Boucher J, Mayes A, Bigham S. Memory in autistic spectrum disorder. *Psychological Bull*. 2012;138:458–496.
- Barnea-Goraly N, Frazier TW, Piacenza L, Minshew NJ, Keshavan MS, Reiss AL, et al. A preliminary longitudinal volumetric MRI study of amygdala and hippocampal volumes in autism. *Prog Neuropsychopharmacol Biol Psychiatry*. 2014;48:124–128.
- Schumann CM, Hamstra J, Goodlin-Jones BL, Lotspeich LJ, Kwon H, Buonocore MH, et al. The amygdala is enlarged in children but not adolescents with autism; the hippocampus is enlarged at all ages. *J Neurosci*. 2004;24:6392–6401.
- Hitti FL, Siegelbaum SA. The hippocampal CA2 region is essential for social memory. *Nature*. 2014;508:88–92.
- Piskrowski RA, Nasrallah K, Diamantopoulou A, Mukai J, Hassan SI, Siegelbaum SA, et al. Age-Dependent Specific Changes in Area CA2 of the Hippocampus and Social Memory Deficit in a Mouse Model of the 22q11.2 Deletion Syndrome. *Neuron*. 2016;89:163–176.
- Avino TA, Barger N, Vargas MV, Carlson EL, Amaral DG, Bauman MD, et al. Neuron numbers increase in the human amygdala from birth to adulthood, but not in autism. *Proc Natl Acad Sci USA*. 2018;115:3710–3715.
- Weir RK, Bauman MD, Jacobs B, Schumann CM. Protracted dendritic growth in the typically developing human amygdala and increased spine density in young ASD brains. *J Comp Neurol*. 2018;526:262–274.
- Bauman MD, Iosif AM, Ashwood P, Braunschweig D, Lee A, Schumann CM, et al. Maternal antibodies from mothers of children with autism alter brain growth and social behavior development in the rhesus monkey. *Transl Psychiatry*. 2013;3:e278.
- Suzuki K, Sugihara G, Ouchi Y, Nakamura K, Futatsubashi M, Takebayashi K, et al. Microglial activation in young adults with autism spectrum disorder. *JAMA Psychiatry*. 2013;70:49–58.
- Vargas DL, Nascimbene C, Krishnan C, Zimmerman AW, Pardo CA. Neuroglial activation and neuroinflammation in the brain of patients with autism. *Ann Neurol*. 2005;57:67–81.
- Hanamsagar R, Alter MD, Block CS, Sullivan H, Bolton JL, Bilbo SD. Generation of a microglial developmental index in mice and in humans reveals a sex difference in maturation and immune reactivity. *Glia*. 2018;66:460.
- Carlezon WA Jr., Kim W, Missig G, Finger BC, Landino SM, Alexander AJ, et al. Maternal and early postnatal immune activation produce sex-specific effects on autism-like behaviors and neuroimmune function in mice. *Sci Rep*. 2019;9:16928.
- Tsilioni I, Patel AB, Pantazopoulos H, Berretta S, Conti P, Leeman SE, et al. IL-37 is increased in brains of children with autism spectrum disorder and inhibits human microglia stimulated by neurotensin. *Proc Natl Acad Sci USA*. 2019;116:21659–21665.
- Velmeshev D, Schirmer L, Jung D, Haessler M, Perez Y, Mayer S, et al. Single-cell genomics identifies cell type-specific molecular changes in autism. *Science*. 2019;364:685–689.
- Haida O, Al Sagheer T, Balbous A, Francheteau M, Matas E, Soria F, et al. Sex-dependent behavioral deficits and neuropathology in a maternal immune activation model of autism. *Transl Psychiatry*. 2019;9:124.
- Werling DM, Geschwind DH. Sex differences in autism spectrum disorders. *Curr Opin Neurol*. 2013;26:146–153.
- Dantzer R. Neuroimmune Interactions: From the Brain to the Immune System and Vice Versa. *Physiol Rev*. 2018;98:477–504.
- Pomin VH. Sulfated glycans in inflammation. *Eur J Med Chem*. 2015;92:353–369.
- Avino TA, Hutsler JJ. Abnormal cell patterning at the cortical gray-white matter boundary in autism spectrum disorders. *Brain Res*. 2010;1360:138–146.
- Wegiel J, Kuchna I, Nowicki K, Imaki H, Wegiel J, Marchi E, et al. The neuropathology of autism: defects of neurogenesis and neuronal migration, and dysplastic changes. *Acta Neuropathol*. 2010;119:755–770.
- Gogolla N, Caroni P, Luthi A, Herry C. Perineuronal nets protect fear memories from erasure. *Science*. 2009;325:1258–1261.
- Maeda N. Proteoglycans and neuronal migration in the cerebral cortex during development and disease. *Front Neurosci*. 2015;9:98.
- Karus M, Ulc A, Ehrlich M, Czopka T, Hennen E, Fischer J, et al. Regulation of oligodendrocyte precursor maintenance by chondroitin sulphate glycosaminoglycans. *Glia*. 2016;64:270–286.
- Pantazopoulos H, Woo T-UW, Lim MP, Lange N, Berretta S. Extracellular Matrix-Glial Abnormalities in the Amygdala and Entorhinal Cortex of Subjects Diagnosed With Schizophrenia. *Arch Gen Psychiatry*. 2010;67:155–166.
- Enwright JF, Sanapala S, Foglio A, Berry R, Fish KN, Lewis DA. Reduced Labeling of Parvalbumin Neurons and Perineuronal Nets in the Dorsolateral Prefrontal Cortex of Subjects with Schizophrenia. *Neuropsychopharmacology*. 2016;41:2206–2214.
- Guan J, Cai JJ, Ji G, Sham PC. Commonality in dysregulated expression of gene sets in cortical brains of individuals with autism, schizophrenia, and bipolar disorder. *Transl Psychiatry*. 2019;9:152.
- Sullivan PF, Magnusson C, Reichenberg A, Boman M, Dalman C, Davidson M, et al. Family history of schizophrenia and bipolar disorder as risk factors for autism. *Arch Gen Psychiatry*. 2012;69:1099–1103.
- Ma D, Salyakina D, Jaworski JM, Konidari I, Whitehead PL, Andersen AN, et al. A genome-wide association study of autism reveals a common novel risk locus at 5p14.1. *Ann Hum Genet*. 2009;73:263–273.
- Wang K, Zhang H, Ma D, Bucan M, Glessner JT, Abrahams BS, et al. Common genetic variants on 5p14.1 associate with autism spectrum disorders. *Nature*. 2009;459:528–533.
- Weiss LA, Arking DE. Gene Discovery Project of Johns H, the Autism C, Daly MJ, Chakravarti A. A genome-wide linkage and association scan reveals novel loci for autism. *Nature*. 2009;461:802–808.
- Hussman JP, Chung RH, Griswold AJ, Jaworski JM, Salyakina D, Ma D, et al. A noise-reduction GWAS analysis implicates altered regulation of neurite outgrowth and guidance in autism. *Mol Autism*. 2011;2:1.
- Anney R, Klei L, Pinto D, Regan R, Conroy J, Magalhaes TR, et al. A genome-wide scan for common alleles affecting risk for autism. *Hum Mol Genet*. 2010;19:4072–4082.
- Abdallah MW, Pearce BD, Larsen N, Greaves-Lord K, Norgaard-Pedersen B, Hougaard DM, et al. Amniotic fluid MMP-9 and neurotrophins in autism spectrum disorders: an exploratory study. *Autism Res*. 2012;5:428–433.
- Slaker ML, Jorgensen ET, Hegarty DM, Liu X, Kong Y, Zhang F, et al. Cocaine Exposure Modulates Perineuronal Nets and Synaptic Excitability of Fast-Spiking Interneurons in the Medial Prefrontal Cortex. *eNeuro*. 2018;5:ENEURO.0221-18.2018.
- Macke EL, Henningsen E, Jessen E, Zornwalde NA, Landowski M, Western DE, et al. Loss of Chondroitin Sulfate Modification Causes Inflammation and Neurodegeneration in skt Mice. *Genetics*. 2020;214:121–134.
- Blacktop JM, Sorg BA. Perineuronal nets in the lateral hypothalamus area regulate cue-induced reinstatement of cocaine-seeking behavior. *Neuropsychopharmacology*. 2018;44:850–858.
- Morawski M, Bruckner G, Jager C, Seeger G, Arendt T. Neurons associated with aggregan-based perineuronal nets are protected against tau pathology in subcortical regions in Alzheimer's disease. *Neuroscience*. 2010;169:1347–1363.
- Baig S, Wilcock GK, Love S. Loss of perineuronal net N-acetylgalactosamine in Alzheimer's disease. *Acta Neuropathol*. 2005;110:393–401.
- Jung M, Ma Y, Iyer RP, DeLeon-Pennell KY, Yabluchansky A, Garrett MR, et al. IL-10 improves cardiac remodeling after myocardial infarction by stimulating M2 macrophage polarization and fibroblast activation. *Basic Res Cardiol*. 2017;112:33.

43. Dobin A, Davis CA, Schlesinger F, Drenkow J, Zaleski C, Jha S, et al. STAR: ultrafast universal RNA-seq aligner. *Bioinformatics*. 2013;29:15–21.
44. Patro R, Duggal G, Love MI, Irizarry RA, Kingsford C. Salmon provides fast and bias-aware quantification of transcript expression. *Nat Methods*. 2017;14:417–419.
45. Love MI, Huber W, Anders S. Moderated estimation of fold change and dispersion for RNA-seq data with DESeq2. *Genome Biol*. 2014;15:550.
46. Wu T, Hu E, Xu S, Chen M, Guo P, Dai Z, et al. clusterProfiler 4.0: A universal enrichment tool for interpreting omics data. *Innov (Camb)*. 2021;2:100141.
47. Yu G, He QY. ReactomePA: an R/Bioconductor package for reactome pathway analysis and visualization. *Mol Biosyst*. 2016;12:477–479.
48. Schmittgen TD, Livak KJ. Analyzing real-time PCR data by the comparative C(T) method. *Nat Protoc*. 2008;3:1101–1108.
49. Clark SM, Pocivavsek A, Nicholson JD, Notarangelo FM, Langenberg P, McMahon RP, et al. Reduced kynurenine pathway metabolism and cytokine expression in the prefrontal cortex of depressed individuals. *J Psychiatry Neurosci*. 2016;41:386–394.
50. Bauer DE, Haroutunian V, McCullumsmith RE, Meador-Woodruff JH. Expression of four housekeeping proteins in elderly patients with schizophrenia. *J Neural Transm*. 2009;116:487–491.
51. Jolly S, Lang V, Koelzer VH, Sala Frigerio C, Magno L, Salinas PC, et al. Single-Cell Quantification of mRNA Expression in The Human Brain. *Sci Rep*. 2019;9:12353.
52. Rocco BR, Oh H, Shukla R, Mechawar N, Sibille E. Fluorescence-based cell-specific detection for laser-capture microdissection in human brain. *Sci Rep*. 2017;7:14213.
53. Brandau DT, Lund M, Cooley LD, Sanger WG, Butler MG. Autistic and dysmorphic features associated with a submicroscopic 2q33.3-q34 interstitial deletion detected by array comparative genomic hybridization. *Am J Med Genet Part A*. 2008;146A:521–524.
54. Harrington AJ, Bridges CM, Berto S, Blankenship K, Cho JY, Assali A, et al. MEF2C Hypofunction in Neuronal and Neuroimmune Populations Produces MEF2C Haploinsufficiency Syndrome-like Behaviors in Mice. *Biol Psychiatry*. 2020;88:488–499.
55. Fassio A, Patry L, Congia S, Onofri F, Piton A, Gauthier J, et al. SYN1 loss-of-function mutations in autism and partial epilepsy cause impaired synaptic function. *Hum Mol Genet*. 2011;20:2297–2307.
56. Oikonomakis V, Kosma K, Mitrakos A, Sofocleous C, Pervanidou P, Syrmou A, et al. Recurrent copy number variations as risk factors for autism spectrum disorders: analysis of the clinical implications. *Clin Genet*. 2016;89:708–718.
57. Coley AA, Gao WJ. PSD95: A synaptic protein implicated in schizophrenia or autism? *Prog Neuropsychopharmacol Biol Psychiatry*. 2018;82:187–194.
58. Greco B, Manago F, Tucci V, Kao HT, Valtorta F, Benfenati F. Autism-related behavioral abnormalities in synapsin knockout mice. *Behav Brain Res*. 2013;251:65–74.
59. Paciorkowski AR, Traylor RN, Rosenfeld JA, Hoover JM, Harris CJ, Winter S, et al. MEF2C Haploinsufficiency features consistent hyperkinesia, variable epilepsy, and has a role in dorsal and ventral neuronal developmental pathways. *Neurogenetics*. 2013;14:99–111.
60. Gross AR, Theoharides TC. Chondroitin sulfate inhibits secretion of TNF and CXCL8 from human mast cells stimulated by IL-33. *Biofactors*. 2019;45:49–61.
61. Theoharides TC, Kavalioti M, Tsiloni I. Mast Cells, Stress, Fear and Autism Spectrum Disorder. *Int J Mol Sci*. 2019;20:3611.
62. Rolls A, Avidan H, Cahalon L, Schori H, Bakalash S, Litvak V, et al. A disaccharide derived from chondroitin sulphate proteoglycan promotes central nervous system repair in rats and mice. *Eur J Neurosci*. 2004;20:1973–1983.
63. Rolls A, Cahalon L, Bakalash S, Avidan H, Lider O, Schwartz M. A sulfated disaccharide derived from chondroitin sulfate proteoglycan protects against inflammation-associated neurodegeneration. *FASEB J*. 2006;20:547–549.
64. Parks WC, Wilson CL, Lopez-Boado YS. Matrix metalloproteinases as modulators of inflammation and innate immunity. *Nat Rev Immunol*. 2004;4:617–629.
65. Muri L, Leppert D, Grandgirard D, Leib SL. MMPs and ADAMs in neurological infectious diseases and multiple sclerosis. *Cell Mol Life Sci*. 2019;76:3097–3116.
66. Rosenberg GA, Cunningham LA, Wallace J, Alexander S, Estrada EY, Grossetete M, et al. Immunohistochemistry of matrix metalloproteinases in reperfusion injury to rat brain: activation of MMP-9 linked to stromelysin-1 and microglia in cell cultures. *Brain Res*. 2001;893:104–112.
67. Cahoy JD, Emery B, Kaushal A, Foo LC, Zamanian JL, Christopherson KS, et al. A transcriptome database for astrocytes, neurons, and oligodendrocytes: a new resource for understanding brain development and function. *J Neurosci*. 2008;28:264–278.
68. Baram D, Vaday GG, Salamon P, Drucker I, Hershkovitz R, Mekori YA. Human mast cells release metalloproteinase-9 on contact with activated T cells: juxtacrine regulation by TNF- α . *J Immunol*. 2001;167:4008–4016.
69. Kanbe N, Tanaka A, Kanbe M, Itakura A, Kurosawa M, Matsuda H. Human mast cells produce matrix metalloproteinase 9. *Eur J Immunol*. 1999;29:2645–2649.
70. Wen TH, Afroz S, Reinhard SM, Palacios AR, Tapia K, Binder DK, et al. Genetic Reduction of Matrix Metalloproteinase-9 Promotes Formation of Perineuronal Nets Around Parvalbumin-Expressing Interneurons and Normalizes Auditory Cortex Responses in Developing Fmr1 Knock-Out Mice. *Cereb Cortex*. 2018;28:3951–3964.
71. Pirbhoy PS, Rais M, Lovelace JW, Woodard W, Razak KA, Binder DK, et al. Acute pharmacological inhibition of matrix metalloproteinase-9 activity during development restores perineuronal net formation and normalizes auditory processing in Fmr1 KO mice. *J Neurochem*. 2020;55:538–558.
72. Reinhard SM, Rais M, Afroz S, Hanania Y, Pendi K, Espinoza K, et al. Reduced perineuronal net expression in Fmr1 KO mice auditory cortex and amygdala is linked to impaired fear-associated memory. *Neurobiol Learn Mem*. 2019;164:107042.
73. Bilousova TV, Dansie L, Ngo M, Aye J, Charles JR, Ethell DW, et al. Minocycline promotes dendritic spine maturation and improves behavioural performance in the fragile X mouse model. *J Med Genet*. 2009;46:94–102.
74. Yamagata M, Sanes JR. Versican in the developing brain: lamina-specific expression in interneuronal subsets and role in presynaptic maturation. *J Neurosci*. 2005;25:8457–8467.
75. Wu Y, Sheng W, Chen L, Dong H, Lee V, Lu F, et al. Versican V1 isoform induces neuronal differentiation and promotes neurite outgrowth. *Mol Biol Cell*. 2004;15:2093–2104.
76. Yang S, Gigout S, Molinaro A, Naito-Matsui Y, Hilton S, Foscarin S, et al. Chondroitin 6-sulphate is required for neuroplasticity and memory in ageing. *Mol Psychiatry*. 2021;26:5658–5668.
77. Charbonnier F, Chanoine C, Cifuentes-Diaz C, Gallien CL, Rieger F, Alliel PM, et al. Expression of the proteoglycan SPOCK during mouse embryo development. *Mech Dev*. 2000;90:317–321.
78. Pantazopoulos H, Katsel P, Haroutunian V, Chelini G, Klengel T, Berretta S. Molecular signature of extracellular matrix pathology in schizophrenia. *Eur J Neurosci*. 2021;53:3960–3987.
79. Cross-Disorder Group of the Psychiatric Genomics C, Lee SH, Ripke S, Neale BM, Faraone SV, Purcell SM, et al. Genetic relationship between five psychiatric disorders estimated from genome-wide SNPs. *Nat Genet*. 2013;45:984–994.
80. Ogawa T, Hagihara K, Suzuki M, Yamaguchi Y. Brevican in the developing hippocampal fimbria: differential expression in myelinating oligodendrocytes and adult astrocytes suggests a dual role for brevican in central nervous system fiber tract development. *J Comp Neurol*. 2001;432:285–295.
81. Lipton SA, Li H, Zaremba JD, McKercher SR, Cui J, Kang YJ, et al. Autistic phenotype from MEF2C knockout cells. *Science*. 2009;323:208.
82. Mikhail FM, Lose EJ, Robin NH, Descartes MD, Rutledge KD, Rutledge SL, et al. Clinically relevant single gene or intragenic deletions encompassing critical neurodevelopmental genes in patients with developmental delay, mental retardation, and/or autism spectrum disorders. *Am J Med Genet Part A*. 2011;155A:2386–2396.
83. Harrington AJ, Raissi A, Rajkovich K, Berto S, Kumar J, Molinaro G, et al. MEF2C regulates cortical inhibitory and excitatory synapses and behaviors relevant to neurodevelopmental disorders. *eLife*. 2016;5:e20059.
84. Glasson EJ, Bower C, Petterson B, de Klerk N, Chaney G, Hallmayer JF. Perinatal factors and the development of autism: a population study. *Arch Gen Psychiatry*. 2004;61:618–627.
85. Gardener H, Spiegelman D, Buka SL. Perinatal and neonatal risk factors for autism: a comprehensive meta-analysis. *Pediatrics*. 2011;128:344–355.
86. Li Y, Missig G, Finger BC, Landino SM, Alexander AJ, Mokler EL, et al. Maternal and Early Postnatal Immune Activation Produce Dissociable Effects on Neurotransmission in mPFC-Amygdala Circuits. *J Neurosci*. 2018;38:3358–3372.
87. Giovanoli S, Weber-Stadlbauer U, Schedlowski M, Meyer U, Engler H. Prenatal immune activation causes hippocampal synaptic deficits in the absence of overt microglia anomalies. *Brain Behav Immun*. 2016;55:25–38.
88. Oh-Nishi A, Obayashi S, Sugihara I, Minamoto T, Suhara T. Maternal immune activation by polyriboinosinic-polyribocytidilic acid injection produces synaptic dysfunction but not neuronal loss in the hippocampus of juvenile rat offspring. *Brain Res*. 2010;1363:170–179.
89. Hasel P, Rose IVL, Sadick JS, Kim RD, Liddel SA. Neuroinflammatory astrocyte subtypes in the mouse brain. *Nat Neurosci*. 2021;24:1475–1487.
90. Vlkolinsky R, Siggins GR, Campbell IL, Krucker T. Acute exposure to CXCL chemokine ligand 10, but not its chronic astroglial production, alters synaptic plasticity in mouse hippocampal slices. *J Neuroimmunol*. 2004;150:37–47.
91. Jourquin J, Tremblay E, Bernard A, Charton G, Chailan FA, Marchetti E, et al. Tissue inhibitor of metalloproteinases-1 (TIMP-1) modulates neuronal death, axonal plasticity, and learning and memory. *Eur J Neurosci*. 2005;22:2569–2578.
92. Tsilibary E, Tzinia A, Radenovic L, Stamenkovic V, Lebitko T, Mucha M, et al. Neural ECM proteases in learning and synaptic plasticity. *Prog Brain Res*. 2014;214:135–157.
93. Han RT, Vainchtein ID, Schlachetzki JCM, Cho FS, Dorman LC, Ahn E, et al. Microglial pattern recognition via IL-33 promotes synaptic refinement in developing corticothalamic circuits in mice. *J Exp Med*. 2023;220:e20220605.
94. Tabet A, Apra C, Stranahan AM, Anikeeva P. Changes in Brain Neuroimmunology Following Injury and Disease. *Front Integr Neurosci*. 2022;16:894500.
95. Coll-Tane M, Gong NN, Belfer SJ, van Renssen LV, Kurtz-Nelson EC, Szuperak M, et al. The CHD8/CHD7/Kismet family links blood-brain barrier glia and serotonin to ASD-associated sleep defects. *Sci Adv*. 2021;7:eabe2626.

96. Fiorentino M, Sapone A, Senger S, Camhi SS, Kadzielski SM, Buie TM, et al. Blood-brain barrier and intestinal epithelial barrier alterations in autism spectrum disorders. *Mol Autism*. 2016;7:49.
97. Ikeda Y, Aihara K, Yoshida S, Iwase T, Tajima S, Izawa-Ishizawa Y, et al. Heparin cofactor II, a serine protease inhibitor, promotes angiogenesis via activation of the AMP-activated protein kinase-endothelial nitric-oxide synthase signaling pathway. *J Biol Chem*. 2012;287:34256–34263.
98. Tollefsen DM. Heparin cofactor II modulates the response to vascular injury. *Arterioscler Thromb Vasc Biol*. 2007;27:454–460.
99. O'Brown NM, Patel NB, Hartmann U, Klein AM, Gu C, Megason SG. The secreted neuronal signal Spock1 regulates the blood-brain barrier. *bioRxiv*. 2021. <https://doi.org/10.1101/2021.10.13.464312>.

ACKNOWLEDGEMENTS

We thank the NIH NeuroBioBank (<https://neurobiobank.nih.gov/>) for making the human brain samples available. The authors deeply appreciate the invaluable contributions made by the families consenting to donate brain tissue. The work performed through the UMMC Molecular and Genomics Facility is supported, in part, by funds from the NIGMS, including the Molecular Center of Health and Disease (P20GM144041), Mississippi INBRE (P20GM103476) and Obesity, Cardiorenal and Metabolic Diseases- COBRE(P30GM149404). Funding for these studies was also provided by the Inflammation Healing Foundation.

AUTHOR CONTRIBUTIONS

HP designed the studies, analyzed data, and wrote the manuscript. LER contributed to study design, collected data, analyzed data, and wrote the manuscript. MRG and BG contributed to study design, data collection, and manuscript preparation. JH, EB, KH, JV, RB, RA, and AG contributed to data collection. KS, MV, BM, and LC contributed to data analysis and manuscript preparation. TT contributed to study design, data interpretation, and manuscript preparation. All authors contributed to the article and approved the submitted version.

COMPETING INTERESTS

The authors declare no competing interests.

ADDITIONAL INFORMATION

Supplementary information The online version contains supplementary material available at <https://doi.org/10.1038/s41380-024-02441-8>.

Correspondence and requests for materials should be addressed to Harry Pantazopoulos.

Reprints and permission information is available at <http://www.nature.com/reprints>

Publisher's note Springer Nature remains neutral with regard to jurisdictional claims in published maps and institutional affiliations.



Open Access This article is licensed under a Creative Commons Attribution 4.0 International License, which permits use, sharing, adaptation, distribution and reproduction in any medium or format, as long as you give appropriate credit to the original author(s) and the source, provide a link to the Creative Commons licence, and indicate if changes were made. The images or other third party material in this article are included in the article's Creative Commons licence, unless indicated otherwise in a credit line to the material. If material is not included in the article's Creative Commons licence and your intended use is not permitted by statutory regulation or exceeds the permitted use, you will need to obtain permission directly from the copyright holder. To view a copy of this licence, visit <http://creativecommons.org/licenses/by/4.0/>.

© The Author(s) 2024